Research article JHEP|Reports

Hepatocyte proteomes reveal the role of protein disulfide isomerase 4 in alpha 1-antitrypsin deficiency

Authors

Esra Karatas, Anne-Aurélie Raymond, Céline Leon, Jean-William Dupuy, Sylvaine Di-Tommaso, Nathalie Senant, Sophie Collardeau-Frachon, Mathias Ruiz, Alain Lachaux, Frédéric Saltel, Marion Bouchecareilh

Correspondence

marionb@ibgc.cnrs.fr (M. Bouchecareilh).

Graphical abstract

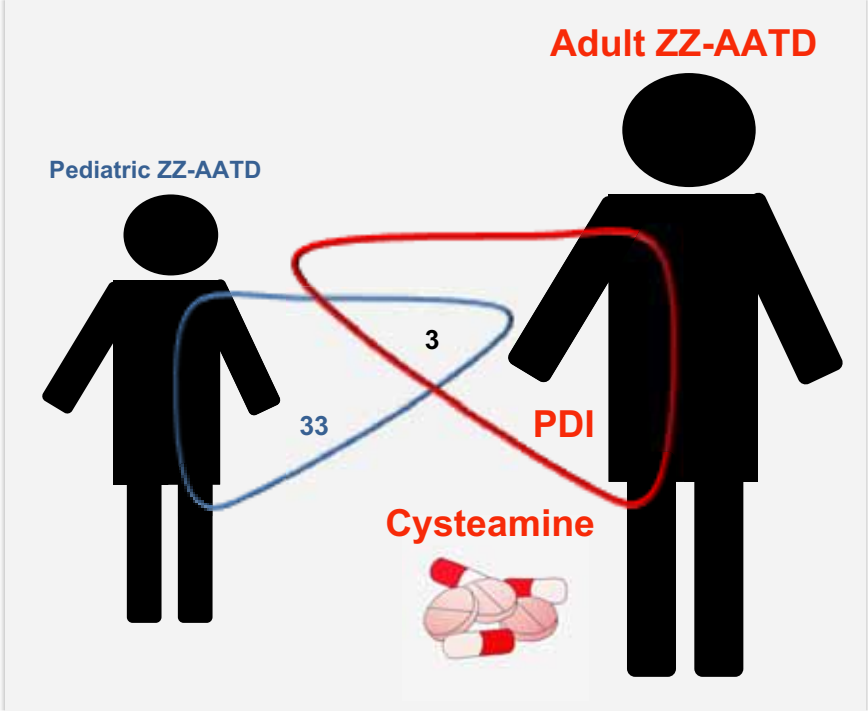

Highlights

- PDIA4 is upregulated and involved in alpha 1-antitrypsin deficiency (AATD)-mediated liver disease in adults.
- Knockdown of PDIA4 by siRNA or inhibition upon cysteamine treatment leads to improvements in features of AATD.
- RNA interference against PDIA4 or cysteamine represent approaches for treatment of AATD-mediated liver disease.

Lay summary

Protein disulfide isomerase (PDI) family members, and particularly PDIA4, are upregulated and involved in alpha 1-antitrypsin deficiency (AATD)-mediated liver disease in adults. PDI inhibition upon cysteamine treatment leads to improvements in features of AATD and hence represents a therapeutic approach for treatment of AATD-mediated liver disease.

https://doi.org/10.1016/j.jhepr.2021.100297

Research article

JHEP|Reports

Hepatocyte proteomes reveal the role of protein disulfide isomerase 4 in alpha 1-antitrypsin deficiency

Esra Karatas,[1] Anne-Aurélie Raymond,[1,2] Céline Leon,[1] Jean-William Dupuy,[3] Sylvaine Di-Tommaso,[2] Nathalie Senant,[4] Sophie Collardeau-Frachon,[5,6,8] Mathias Ruiz,[6,7,8] Alain Lachaux,[6,7,8] Frédéric Saltel,[1,2] Marion Bouchecareilh[1,*]

[1]*University of Bordeaux, CNRS, INSERM, BaRITOn, U1053, Bordeaux, France;* [2]*Oncoprot, University of Bordeaux, INSERM, TBM-Core, UMS 3427, US 5, Bordeaux, France;* [3]*University of Bordeaux, Plateforme Protéome, Bordeaux, France;* [4]*Plateforme d'histopathologie, TBM-Core US 005, Bordeaux, France;* [5]*Department of Pathology, Hôpital Femme Mère Enfant, Hospices Civils de Lyon, Lyon, France;* [6]*Hépatologie, Gastroentérologie et Nutrition pédiatriques, Centre de référence de l'atrésie des voies biliaires et cholestases génétiques, Hôpital Femme Mère Enfant, Hospices Civils de Lyon, Lyon, France;* [7]*European Reference Network on Hepatological Diseases (ERN RARE-LIVER), Hamburg, Germany;* [8]*Faculté de Médecine Lyon-Est, Université Claude Bernard Lyon 1, Lyon, France*

JHEP Reports **2021.** https://doi.org/10.1016/j.jhepr.2021.100297

Background & Aims: A single point mutation in the Z-variant of alpha 1-antitrypsin (Z-AAT) alone can lead to both a protein folding and trafficking defect, preventing its exit from the endoplasmic reticulum (ER), and the formation of aggregates that are retained as inclusions within the ER of hepatocytes. These defects result in a systemic AAT deficiency (AATD) that causes lung disease, whereas the ER-retained aggregates can induce severe liver injury in patients with ZZ-AATD. Unfortunately, therapeutic approaches are still limited and *liver transplantation* represents the *only curative treatment* option. To overcome this limitation, a better understanding of the molecular basis of ER aggregate formation could provide new strategies for therapeutic intervention.

Methods: Our functional and omics approaches here based on human hepatocytes from patients with ZZ-AATD have enabled the identification and characterisation of the role of the protein disulfide isomerase (PDI) A4/ERP72 in features of AATD-mediated liver disease.

Results: We report that 4 members of the PDI family (PDIA4, PDIA3, P4HB, and TXNDC5) are specifically upregulated in ZZ-AATD liver samples from adult patients. Furthermore, we show that only PDIA4 knockdown or alteration of its activity by cysteamine treatment can promote Z-AAT secretion and lead to a marked decrease in Z aggregates. Finally, detailed analysis of the Z-AAT interactome shows that PDIA4 silencing provides a more conducive environment for folding of the Z mutant, accompanied by reduction of Z-AAT-mediated oxidative stress, a feature of AATD-mediated liver disease.

Conclusions: PDIA4 is involved in AATD-mediated liver disease and thus represents a therapeutic target for inhibition by drugs such as cysteamine. PDI inhibition therefore represents a potential therapeutic approach for treatment of AATD.

Lay summary: Protein disulfide isomerase (PDI) family members, and particularly PDIA4, are upregulated and involved in alpha 1-antitrypsin deficiency (AATD)-mediated liver disease in adults. PDI inhibition upon cysteamine treatment leads to improvements in features of AATD and hence represents a therapeutic approach for treatment of AATD-mediated liver disease.

Introduction

Alpha 1-antitrypsin deficiency (AATD) is a rare genetic disorder that leads to lung and liver diseases during childhood and adulthood.[1] This deficiency results from point mutations in the *SERPINA1* gene that affect the correct folding of its encoded protein, alpha 1-antitrypsin (AAT). This leads to retention of AAT in the endoplasmic reticulum (ER) of hepatocytes.[2] Over 100 mutant AAT proteins have already been identified, and among these the most severe and most common disease-causing allele is the Z variant.[3–5] This variant is caused by mutation of glutamate to lysine at position 342. This amino acid change not only leads to inefficient export of soluble Z-AAT monomers out of the ER, but also contributes to the formation of insoluble polymers that accumulate in the ER. Approximately 10% of the ZZ population develop clinically significant liver disease that can progress to end-stage liver disease requiring liver transplantation.[3,4] This clinical outcome is closely associated with Z-AAT aggregate load in hepatocytes.[6]

Aggregate formation is caused by Z-variant mutation that induces β-sheet opening, favouring partial loop insertion of another AAT molecule and formation of a loop-sheet dimer that *then extends to form aggregates*.[7] This model was recently

Keywords: Alpha 1-antitrypsin deficiency; Liver damage; Protein disulfide isomerase; PDIA4; Cysteamine; Treatment.
Received 12 October 2020; received in revised form 6 April 2021; accepted 9 April 2021; available online 24 April 2021

* Corresponding author. Address: INSERM CNRS U1053 BaRITon Bat 1A 2eme étage 146, Rue Léo Saignat 33076 Bordeaux, France. Tel: +33-557571121
E-mail address: marionb@ibgc.cnrs.fr (M. Bouchecareilh).

developed by Ronzoni *et al.*[8] who observed that Z-AAT aggregates are also caused by the formation of aberrant intra- and inter-molecular disulfide bonding with other AAT variants and potentially with other ER-resident proteins. These disulfide bonds stabilise aberrant AAT conformations and contribute to its pathogenic ER retention and impede its transport to distal compartments of the secretory pathway.[8]

Disulfides are covalent bonds produced by the oxidation of 2 free thiols. In proteins they form between 2 cysteine residues. This rate-limiting step takes place in the ER and plays an important role in protein folding and stability.[9–11] The process is assisted and catalysed by members of the protein disulfide isomerase (PDI) family that are responsible for the formation, breakage, and rearrangement of disulfide bonds in proteins (*e.g.* isomerase/oxidative refolding/reductase activities). Independently of their disulfide isomerase activity, some PDIs recognise misfolded polypeptide regions via their chaperone-like substrate domain, thereby preventing protein aggregation.[9–11] In addition, it is also well appreciated that PDI can cause oxidative stress by increasing, for instance, the levels of reactive oxygen species (ROS), a major inducer of oxidative damage and stress during protein disulfide bond formation.[12]

Members of the *PDI family* represent the most abundant proteins among the ER lumen proteins.[9–11] Regarding AAT, it has been shown in mouse models that Z-aggregate excess can induce a shift in the activity of P4HB (prolyl 4-hydroxylase subunit beta/PDIA1, one of the PDI members), leading to a change in the ER redox balance.[13] Moreover, knockdown of the oxidoreductase Ero1L, a PDI co-factor, corrects the Z-AAT trafficking defect.[14] Finally, oxidative stress has been identified as a contributing factor in the development of liver disease in a mouse model of AATD.[15] Altogether, these data suggest that the PDI family could be involved in the ER retention of Z-AAT and in the cellular stress pathways associated with ER accumulation of Z-AAT, both mechanisms thus potentially underlying the lung and liver diseases associated with AATD.

In this study we report the upregulation of PDIA4 (protein disulfide isomerase family A member 4/ERP70/ERP72) in hepatocytes from adult patients with ZZ-AATD and demonstrate that PDIA4 silencing corrects the defects associated with Z-AAT-mediated AATD (traffic, secretion, aggregation). Further characterisation enabled us to demonstrate that PDIA4-dependent correction functions, at least in part, by modulating the Z-AAT interactome. This is via promoting Z-AAT interactions that form a more conducive protein environment for the folding and trafficking of the Z mutant, but also by decreasing the oxidative stress associated with Z-AATD. Accordingly, inhibition of PDI following treatment with the FDA-approved cysteamine drug led to a reduction in Z-AAT insoluble forms, accompanied by a decrease in oxidative stress associated with AATD-mediated liver disease.

Materials and methods

Materials

PDI inhibitors (16F16, bacitracin, cystamine, cysteamine, hypotaurine, PACMA 31) and cycloheximide were purchased from Sigma-Aldrich (Saint-Louis, Missouri, USA), P1 was obtained from Tocris Bioscience and tunicamycin was purchased from Calbiochem (San Diego, CA, USA). These inhibitors were dissolved in DMSO (16F16/cystamine/cysteamine/PACMA 31/P1/tunicamycin/cycloheximide) or in cell culture medium (bacitracin/hypotaurine). Small RNA interference [siRNA] were obtained from Ambion (Austin, TX, USA) and plasmids from Origene (Rockville, MD, USA). All antibodies and siRNA used in this work have been described in tables included in the Supplementary data. These tables indicate providers and catalogue number of each antibody and also the sequences of all the siRNA (Table S5).

Study approval

All the human samples were obtained from the 'Tissu-Tumorothèque Est, CRB-HCL' according to standard protocols and written informed consent was obtained from all participants or their legal guardians included in the study. These samples are from subjects homozygous for the Z or wild-type (WT) alleles of *SERPINA1* (Table S1). Paediatric liver control samples were obtained from patients with diagnoses of *oxalosis*. The study protocol conforms to the ethical guidelines of the 1975 Declaration of Helsinki as reflected in *a priori* approval by the institution's human research committee.

Statistical analysis

All experiments were performed in at least 3 independent replicates. Data were reported as the mean ± SEM of at least 3 experiments. Statistical analyses were performed using the GraphPad Prism 5.0 application (GraphPad Software, San Diego, CA, USA). The differential protein expression between the cell lines was validated by a *t* test $^{*}p < 0.05$. One-way ANOVA analysis of variance followed by the Bonferroni post-test was used for the comparison of means in experiments containing 3 groups or more.

Proteomic analysis for interactome

Steps of sample preparation and protein digestion were performed as previously described.[16] Online nanoLC-MS/MS analyses were performed using an ultimate 3000 RSLC Nano-UPHLC system (Thermo Fisher Scientific, Waltham, Massachusetts, USA) coupled to a nanospray Q-Exactive hybrid quadruplole-Orbitrap mass spectrometer (Thermo Scientific). Each peptide extract was loaded on a 300 μm IDx5 mm PepMap C_{18} precolumn (Thermo Scientific) at a flow rate of 10 μl/min. After 3 min desalting, peptides were online separated on a 75 μm IDx25 cm C_{18} Acclaim PepMap® RSLC column (Thermo Scientific) with a 4–40% linear gradient of solvent B (0.1% formic acid in 80% acetonitrile [ACN]) in 108 min. The separation flow rate was set at 300 nl/min. The mass spectrometer operated in positive ion mode at a 1.8 kV needle voltage. Data were acquired using Xcalibur 3.1 software (Thermo Fisher Scientific Inc., Waltham, MA, USA) in a data-dependent mode. MS scans (m/z 350–1600) were recorded at a resolution of R = 70,000 (@ m/z 200) and an AGC target of $3x10^6$ ions collected within 100 ms. Dynamic exclusion was set to 30 s and the top 12 ions were selected from fragmentation in HCD mode. MS/MS scans with a target value of $1x10^5$ ions were collected with a maximum fill time of 100 ms and a resolution of R = 17,500. Additionally, only +2 and +3 charged ions were selected for fragmentation. Other settings were as follows: no sheath and no auxiliary gas flow, heated capillary temperature, 200°C; normalised HCD collision energy of 27% and an isolation width of 2 m/z. Mascot 2.5 algorithm through Proteome Discoverer 1.4 Software (Thermo Fisher Scientific Inc., , CA, USA) was used in batch mode by searching against the UniProt *Homo sapiens* database (70,632 entries, Reference Proteome Set, release date: June 29, 2016) from the

http://www.uniprot.org/ website. Two missed enzyme cleavages were allowed. Mass tolerances in MS and MS/MS were set to 10 ppm and 0.02 Da. Oxidation of methionine, acetylation of lysine, and deamidation of asparagine and glutamine were searched as dynamic modifications. Carbamidomethylation on cysteine was searched as static modification. Raw LC-MS/MS data were imported in proline studio[17] for feature detection, alignment, and quantification. Proteins identification was accepted only with at least 2 specific peptides with a rank = 1 and with a protein false discovery rate value less than 1.0% calculated using the 'decoy' option in Mascot. Label-free quantification of MS1 level by extracted ion chromatograms (XIC) was carried out with parameters indicated previously.[16] We considered a protein enriched by co-immunoprecipitation if its immunoprecipitation ratio to a control was ≥2. The mass spectrometry proteomics data have been deposited to the proteomeXchange Consortium via the PRIDE[18] partner repository with the dataset identifier PXD022994.

Hepatocytes proteome

Microdissected tissues were incubated in a Tris-HCl pH 6.8 solution for 2 h at 95°C. Samples were loaded on a 10% acrylamide SDS-PAGE gel. Migration was stopped when the samples entered the resolving gel and the proteins were visualised by colloidal blue staining. Steps of sample preparation and protein digestion were performed as previously described.[16] Online nanoLC-MS/MS analyses were performed using an ultimate 3000 RSLC Nano-UPHLC system (Thermo Scientific) coupled to a nanospray Orbitrap Fusion™ Lumos™ Tribrid™ Mass Spectrometer (Thermo Fisher Scientific). Each peptide extract was loaded on a 300 μm IDx5 mm PepMap C_{18} precolumn (Thermo Scientific) at a flow rate of 10 μl/min. After a 3-min desalting step, peptides were separated on a 50-cm EasySpray column (75 μm ID, 2 μm C_{18} beads, 100 Å pore size, ES803, Thermo Fisher Scientific) with a 4–40% linear gradient of solvent B (0.1% formic acid in 80% ACN) in 55 min. The separation flow rate was set at 300 nl/min. The mass spectrometer operated in positive ion mode at a 2.0 kV needle voltage. Data were acquired using Xcalibur 4.1 software in a data-dependent mode. MS scans (m/z 375–1,500) were recorded at a resolution of R = 120,000 (@ m/z 200) and an AGC target of $4x10^5$ ions collected within 50 ms, followed by a top speed duty cycle of up to 3 s for MS/MS acquisition. Precursor ions (2–7 charge states) were isolated in the quadrupole with a mass window of 1.6 Th and fragmented with HCD @30% normalised collision energy. MS/MS data was acquired in the orbitrap cell with a resolution of R = 30,000 (@m/z 200), AGC target of $5x10^4$ ions and a maximum injection time of 100 ms. Selected precursors were excluded for 60 s. Mascot 2.5 algorithm through Proteome Discoverer 2.4 Software (Thermo Scientific) was used in batch mode by searching against the UniProt *Homo sapiens* database (73,950 entries, Reference Proteome Set, release date: November 17, 2018) from the http://www.uniprot.org/ website. Two missed enzyme cleavages were allowed. Mass tolerances in MS and MS/MS were set to 10 ppm and 0.02 Da. Oxidation of methionine, acetylation of lysine, and deamidation of asparagine and glutamine were searched as dynamic modifications. Carbamidomethylation on cysteine was searched as static modification. Raw LC-MS/MS data were imported in proline studio[17] for feature detection, alignment, and quantification. Protein identification was accepted only with at least 2 specific peptides with a pretty rank = 1 and with a protein FDR value less than 1.0% calculated using the 'decoy' option in Mascot. Label-free quantification of MS1 level by extracted ion chromatograms (XIC) was carried out with parameters indicated previously[16] The normalisation was carried out on median of ratios. The inference of missing values was applied with 5% of the background noise. The mass spectrometry proteomics data have been deposited to the ProteomeXchange consortium via the PRIDE[18] partner repository with the dataset identifier PXD022994.

RNA isolation, qRT-PCR, Western blotting, and immunohistochemistry (IHC) analysis were performed as described in the Supplementary Materials and methods.

Results

The PDI family is upregulated in liver samples from adults with AATD

AATD-mediated liver disease displays a biphasic pattern with the first peak in early childhood and the second peak in adulthood (50–65 years of age). It represents the most common inherited metabolic disease leading to liver transplantation.[19] However, according to several existing transplantation databases in the USA, over the past 20 years adults have accounted for a larger proportion of patients having undergone liver transplantation for this diagnosis compared with children.[19,20] Consequently, we aimed to identify factors and potential PDIs underlying the outcome of AATD-mediated liver disease in adults. To do this, we performed an *in situ* proteomic analysis combining laser microdissection of hepatocytes and mass spectrometry analysis on human formalin-fixed paraffin-embedded (FFPE) liver tissues[16] from 4 paediatric and 4 adult patients with ZZ-AATD (referred to as ZZ patients) that underwent liver transplantation (Table S1). For comparison we performed the same analysis on 3 and 4 WT paediatric and adult samples, respectively. Overall, we were able to compare proteins differentially expressed in paediatric *vs*. adult patients with ZZ-AATD. Protein expression was considered a potential marker if the protein count ratio in ZZ *vs.* WT was ≤0.5 or ≥2. Statistical analysis revealed that 65 proteins were exclusively upregulated in adult ZZ patients (Fig. 1A and Table S2). Kyoto Encyclopedia of Genes and Genomes (KEGG) analyses on these 65 proteins revealed that the most enriched and significant network was related to 'protein processing in the endoplasmic reticulum' (Fig. S1A). More precisely, in agreement with gene ontology molecular function analysis, the 12 proteins that constitute this network (Fig. S1A) belong to subnetworks associated with protein disulfide isomerase activity (GO: 0003756) (Fig. S1B). Among these proteins are 4 PDI members: PDIA4, PDIA3 (protein disulfide isomerase family A member 3/ERP57), P4HB (prolyl 4-hydroxylase subunit beta/PDIA1), and TXNDC5 (thioredoxin domain containing 5/PDIA15). These were found upregulated in adult ZZ patients (adults) compared with paediatric ZZ patients (children) (Fig. 1B). These results suggest that PDI members are involved in adult Z-AATD-mediated liver disease.

PDIA4 is involved in Z-AAT biogenesis: traffic, secretion, and aggregation

We took this hypothesis further by addressing the role of PDIA4, PDIA3, P4HB, TXNDC5, and other PDI members in Z-AATD biogenesis by examining the effect of siRNA-mediated knockdown of individual PDIs in 2 cell line models of AATD[14,21,22]: a human bronchial epithelial cell line (IB3), expressing non-tagged WT or Z-AAT (referred to as WT-IB3 and Z-IB3), and a human hepatocellular carcinoma (HCC) cell line (Huh7), expressing N-

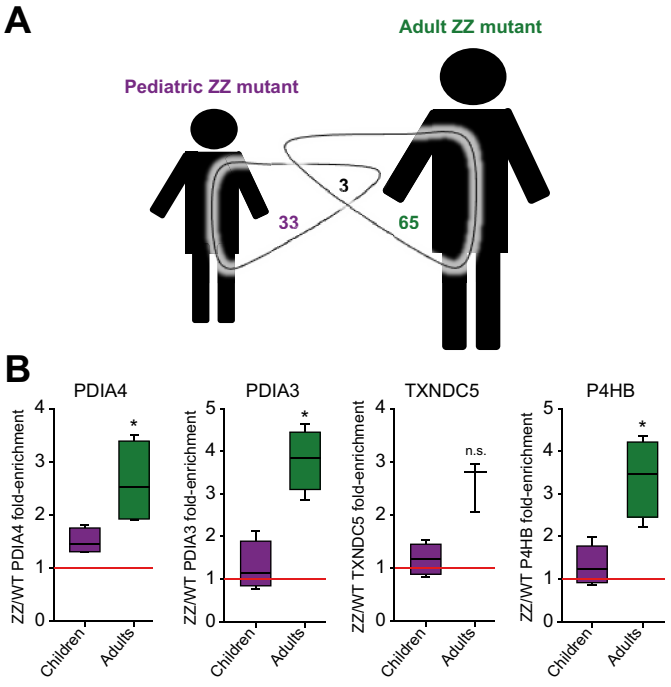

Fig. 1. PDIA4 expression in AATD liver disease. (A) Proportional Venn diagram depicting the overlap of proteins identified in ZZ hepatocytes from adults and children. This Venn diagram indicates the number of proteins significantly upregulated in ZZ paediatric patients (left – 33 upregulated only in hepatocytes of paediatric ZZ patients) and proteins significantly upregulated in ZZ adult patients (right – 65 upregulated only in hepatocytes of ZZ adult patients) and those 3 proteins detected as commonly upregulated in ZZ patients. (B) Expression level of PDIA4, PDIA3, P4HB, and TXNDC5 in hepatocytes from ZZ children (n = 4/left) and ZZ adult (n = 4/right) patients based on data from hepatocyte proteome analysis. In the box plot, the boxes indicate the median and interquartile range of data, and the error bars represent the minimum and maximum values. *p <0.05 as determined by 2-tailed t test using ZZ/WT children ratio as reference. P4HB, prolyl 4-hydroxylase subunit beta/PDIA1; PDIA3, protein disulfide isomerase family A member 3/ERP57; PDIA4, protein disulfide isomerase family A member 4/ERP70/ERP72; TXNDC5: thioredoxin domain containing 5/PDIA15; WT, wild-type; ZZ, *homozygosis* for the *Z* mutant *allele*.

terminal flag-tagged WT or Z-AAT (referred to as WT-Huh7 and Z-Huh7). Following this PDI siRNA screen, we observed that the silencing of numerous PDIs led to a correction of Z-AAT trafficking and secretion (Fig. 2A), thus confirming that several PDIs play a role in mutant Z-AAT retention in the ER. Moreover, we noted that the silencing of PDIA4 exhibited one of the most pronounced effects on the improvement of Z-AAT maturation and secretion relative to control siRNA silencing (scramble [scr]) (Fig. 2A). This result consolidates our identification of PDI expression in the adult ZZ hepatocyte proteome (Fig. 1B). The same result was also observed *using multiple siRNA sequences* and in Z-Huh7 cells (Fig. S1C and siRNA Table S5). We decided thus to focus our study on PDIA4 given it was identified via both of our different approaches (PDI siRNA screening and hepatocyte proteome) (Figs. 1B and 2A).

We next investigated the potential effects of PDIA4 on Z-AAT aggregate load to examine our hypothesis that PDIA4 is involved in Z-AATD-mediated liver disease. To do this, we obtained soluble and insoluble fractions by centrifugation[23] from Z-IB3 cell lysates following control (scr) or PDIA4 silencing using siRNA treatments (Fig. 2B). As expected, we detected a large amount of Z-AAT aggregates following scr treatment (Fig. 2B). In contrast, insoluble Z-AAT fractions showed a significant decrease in PDIA4-silenced cells compared to in scr-treated cells (Fig. 2B). Additionally, PDIA4 silencing corrected Z-AAT-mediated AATD (traffic, secretion, and aggregation) without exhibiting toxicity or any effects on cell proliferation (Fig. 2C).

As we observed beneficial effects on Z-AAT aggregation and secretion in response to PDIA4 silencing, we wanted to determine whether PDIA4 overexpression mediated the opposite effects on features of Z-AAT (aggregation and secretion). As expected, and conversely to what we observed upon PDIA4 silencing, PDIA4 overexpression induced a slight increase in Z-aggregate levels (Fig. S1D) and a decrease in Z-AAT secretion (Fig. S1E). Altogether, these data support that PDIA4 is involved in Z-AATD-mediated liver disease and its inhibition could therefore represent a therapeutic approach for the treatment of AATD.

PDIA4 expression and staining in *liver patients with different aetiology*

To go further and to confirm our proteome analysis (Fig. 1B), we measured and compared the expression of PDIA4 by IHC using an anti-PDIA4 antibody in all the aforementioned AATD patient samples previously analysed by proteomics. PDIA4 expression was slightly detected in both paediatric and adult WT liver samples as well as in paediatric ZZ-AATD liver samples (Fig. 3A and B). Conversely, and as expected, PDIA4 immunostaining was stronger in adult ZZ-AATD liver samples (Fig. 3A and Fig. S2A). Staining was homogeneous and positive for all adult ZZ-FFPE liver samples analysed (Fig. S2A). However, less staining was observed in all paediatric compared with adult ZZ-FFPE liver samples (Fig. S2A). Upregulation of PDIA4 expression was also confirmed using a semi-quantitative analysis of IHC images,[24] PDIA4 expression is statistically significant higher in adult samples than in paediatric samples (Fig. 3B) confirming the upregulation of PDIA4 exclusively found in adult ZZ-FFPE samples (Fig. 1B). Interestingly, this same result was also obtained regarding the other PDIs, P4HB and PDIA3, pinpointed in our proteome analysis (Fig. S2B and C), confirming then our initial analysis (Fig. 1B). We additionally analysed the genome-wide RNA sequencing dataset created by Segeritz *et al.*[25] on human-induced pluripotent stem cells derived from adult patients with ZZ-AATD and the corresponding isogenic WT cells. We also detected an upregulation of PDIA4 in ZZ-hIPSCs with a $\log_2$-fold change of 0.9 for differential gene expression between ZZ and WT (Table S3). Finally, in agreement with another 2 microarray datasets available,[26,27] we also found that PDIA4 mRNA remains unchanged in other liver diseases such as HCC, cholangiocarcinoma, viral hepatitis, non-alcoholic fatty liver disease/non-alcoholic steatohepatitis, fibrosis/cirrhosis, hepatocellular adenoma, and biliary atresia (http://hepamine.digitalbiotop.org/view/1/7?search_key=Vibrio%20Cholerae%20Infection%20(KEGG)) (Fig. S2D). Collectively, these data confirm the role of PDIA4 in Z-AATD-mediated liver disease. PDIA4 could be tested at a larger scale in patients with AATD-mediated liver disease in light of putting it forward as a potential biomarker.

PDIA4 silencing leads to Z-AAT interactome remodelling

To identify the molecular mechanisms by which Z-AAT rescue is achieved, we carried out a cycloheximide-chase analysis to monitor whether Z-AAT trafficking and secretion rescue upon PDIA4 silencing is attributable to a new corrected steady state equilibrium of Z-AAT disposal (Fig. S3A). We did not observe a

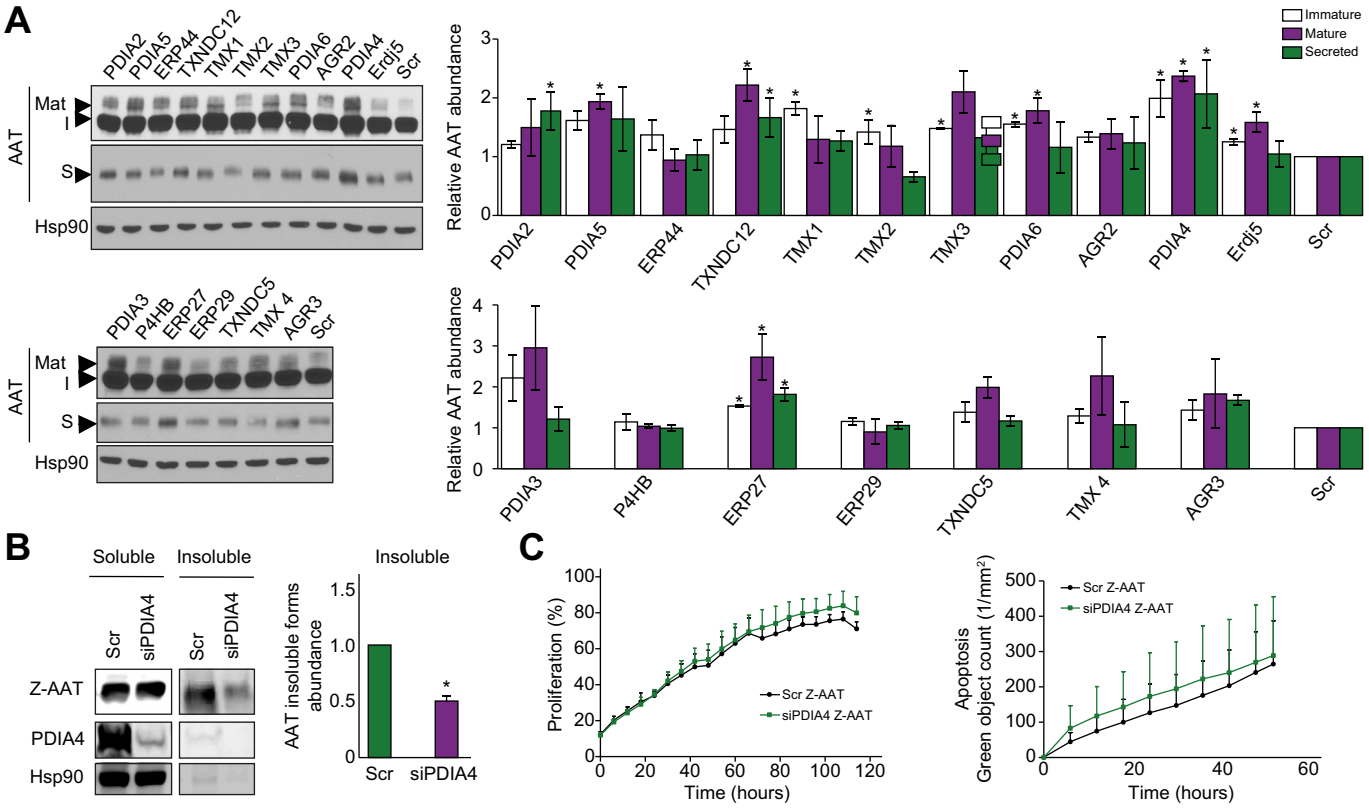

Fig. 2. Correction of Z-AAT biogenesis in response to PDIA4 silencing. (A) Immunoblot analysis of Z-AAT and Hsp90 proteins expression in cell lysates (I, immature; Mat, mature) and culture media (S, secreted) following siRNA-mediated silencing of PDI members in Z-IB3 cells. Traffic of the AAT glycoprotein through the secretory pathway can be monitored by a change in its migration on SDS-PAGE in response to the processing of ER-acquired N-linked oligosaccharides (the immature form: I) during trafficking through the Golgi to generate the slower migrating, mature glycoform (Mat). The latter is secreted in the serum (secreted form: S) by the cell. Quantitative analysis of the level of immature, mature, and secreted Z-AAT forms in response to silencing of the indicated PDI in Z-IB3 cells. Data denote the fold change in Z-AAT expression relative to scramble (scr) control (mean ± SD, n = 3). $^{*}p$ <0.05, $^{**}p$ <0.01, $^{***}p$ <0.001 as determined by 2-tailed *t* test using scr control as the reference. (B) Immunoblot analysis of Z-AAT, PDIA4, and Hsp90 proteins expression in soluble and insoluble (pellet) fractions following siRNA-mediated silencing of PDIA4 (siPDIA4) in Z-IB3 cells and quantification of Z-AAT insoluble forms following siRNA-mediated silencing of PDIA4 (siPDIA4) to scr control. Data denote the fold change in the protein abundance of the indicated Z-AAT aggregated/insoluble form relative to scr control (mean ± SD, n = 3 independent experiments). $^{*}p$ <0.05 as determined by 2-tailed *t* test using scr as reference. (C) IncuCyte® proliferation assay of Z-IB3 (left) cells following scr control (black) or siRNA-mediated silencing of PDIA4 (siPDIA4/green) treatments. Proliferation was quantified in real time using the IncuCyte® live-cell analysis system (see Materials and methods section). IncuCyte® apoptosis assay (right) was performed on Z-IB3 cells upon scr control (black) or siRNA-mediated silencing of PDIA4 (siPDIA4/green) treatments. IncuCyte® caspase-3/7 green reagent was added into the medium and cells were then incubated all along the indicated time (h). The IncuCyte® caspase-3/7 apoptosis assay green reagent couples the activated caspase-3/7 recognition motif (DEVD) to NucView™ 488, a DNA intercalating dye to enable quantification of apoptosis over time (see Supplementary Materials and methods section). Apoptotic cells were quantified in real time using the IncuCyte® live-cell analysis system. ER, endoplasmic reticulum; PDI, protein disulfide isomerase; PDIA4, protein disulfide isomerase family A member 4/ERP70/ERP72; siRNA, small RNA interference; Z-AAT, alpha 1-antitrypsin Z variant.

difference in the stability or disposal of Z-AAT upon PDIA4 silencing (Fig. S3A), suggesting that PDIA4 is not involved in the disposal of the Z mutant. Intracellular co-aggregation and disulfide bonding of Z-AAT with other AAT variants has already been demonstrated,[8] suggesting that this result could correspond to the Z mutant co-aggregating with other ER proteins by forming disulfide bonds, in turn favouring its retention in the ER. Thus, given the role of PDIA4 in formation and rearrangement of protein disulfide bonds, its silencing could prevent Z-AAT co-aggregation by impeding its formation of disulfide bonds with other ER proteins, therefore promoting novel protein associations that could favour Z-AAT trafficking and secretion. To identify these new key interactions that potentially drive silenced PDIA4-mediated Z-AAT rescue, we performed Z-AAT immunoprecipitation (IP) coupled to mass spectrometry analyses for control (scr) or PDIA4 silencing (siPDIA4) (Fig. S3B) in Z-Huh7 cells. We first determined the changes that occurred between scr and siPDIA4 Z-AAT interactomes. These 2 interactomes comprised 850 and 1,051 proteins, respectively, with an overlap of above 82% (Fig. 4A). These 698 shared proteins formed the 'core Z-AAT interactome' and represented direct and indirect Z-AAT interactors. Within this core group we identified 3 PDIs: PDIA4, TXNDC5, and PDIA3. We also previously identified these same PDIs as being upregulated in the adult ZZ hepatocyte proteome (Fig. 1B), reinforcing again that PDI members play an important role in Z-AATD-mediated liver disease.

We confirmed the interaction of Z-AAT with PDIA4 by co-IP in both Z-Huh7 (Fig. 4B) and Z-IB3 cells (Fig. S3C). Interestingly, WT-AAT was not able to bind with PDIA4 (Fig. 4B and Fig. S3C) in the Huh7 cell line model of AATD, suggesting that Z-AAT is a selective substrate for PDIA4 with direct effects on Z-AAT retention in the ER. Thus, modulation of the PDIA4/Z-AAT

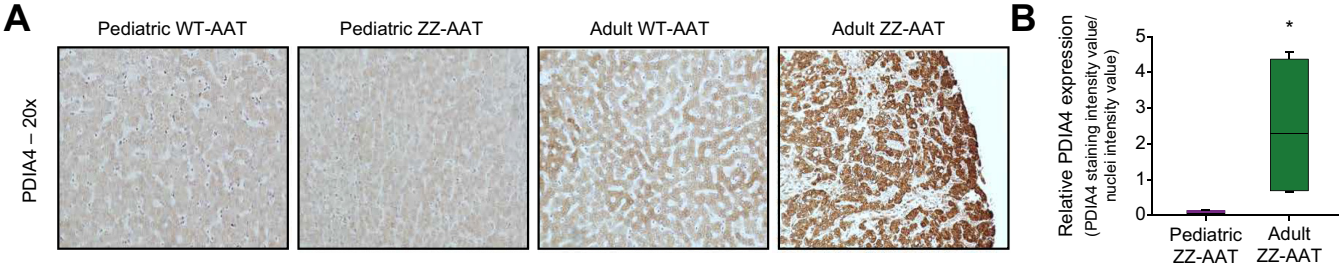

Fig. 3. PDIA4 expression in AATD liver samples. (A) PDIA4 staining in liver tissues using a 20× objective from WT paediatric and adult individuals and ZZ paediatric and adult patients as indicated above the pictures. (B) Semi-quantification of PDIA4 expression of PDIA4 IHC images using imageJ software as previously described.[24] Data denote the fold change in the total PDIA4 staining intensity value normalised by the nuclei intensity value. The average of all PDIA4 staining intensities normalised by nuclei number for all IHC images (n = 32) for each sample (n = 8) give an average value and standard deviation value (mean ± SD, n = 4 independent experiments). AATD, alpha 1-antitrypsin deficiency; IHC, immunohistochemistry; PDIA4, protein disulfide isomerase family A member 4/ERP70/ERP72.

interaction could be a promising strategy for correcting Z-AAT trafficking and secretion defects.

The FKBP10 interactor restores Z-AAT function

We detected an additional 152 and 353 interactors considered as specific in the WT-AAT and Z-AAT interactomes upon PDIA4 silencing, respectively (Fig. 4A). Further gene set enrichment analysis on the interactome data revealed that many of the specific Z-AAT interactors identified following PDIA4 silencing belong to an ER-associated network (Fig. 4C). Indeed, the 67 proteins that constitute this network (Fig. 4C) belong to sub-networks related to protein folding and intracellular transport (Fig. 4D), suggesting that Z-AAT biogenesis is affected by depletion of PDIA4, enhancing its folding and secretion. To determine the most accurate candidates from this list of 353 specific Z-AAT interactors, we only selected proteins harbouring a minimum of 2 peptides identified by mass spectrometry and that co-immunoprecipitated in the 3 independent Z-AAT-siPDIA4 IP experiments. Finally, proteins were selected if their ratio of Z-AAT scr *vs.* Z-AAT PDIA4 silencing was statistically significant and ≤0.5. Candidates that fulfilled these parameters included 18 proteins (Table S4) from which we selected 3: surfeit 4 (SURF4), FK506-binding protein (FKBP) isoform 10 (FKBP10), and SIL1 (nucleotide exchange factor). We selected these 3 proteins based on the fact that they are all ER-resident proteins and are involved in protein folding and secretion. SURF4 and FKBP10 are also required for the trafficking and function of some specific misfolded proteins, such as the ΔF508 mutant of the cystic fibrosis transmembrane conductance regulator (CFTR) protein, a variant that is responsible for the most common clinical presentation of cystic fibrosis (CF).[28,29] We selected the SIL1 protein here as a negative control. Indeed, it has already been shown that SIL1 knockdown has no effect on the degradation of another AAT variant: the null Hong Kong (NHK).[30] Consequently, we performed silencing of these 3 candidates using siRNA and monitored the Z-AAT trafficking pattern in Z-IB3 cells. Knockdown of both SIL1 or SURF4 proteins exhibited minor effects on Z-AAT biogenesis (Fig. S4A), whereas knockdown of FKBP10 led to reduced Z-AAT trafficking and secretion (Fig. S4B). These results suggest that FKBP10 is important for the folding of Z-AAT.

PDI inhibitors rescue the Z-AAT secretion defect

Given that PDI members, and in particular PDIA4, are involved in Z-AATD-mediated liver disease in adults, these candidates are molecular targets of interest for the management of AATD, especially in the prevention and treatment of liver disorders associated with AATD. Accordingly, we examined the potential therapeutic strategy of targeting PDIs by testing the effects of PDI inhibitor (PDIi) treatments (16F16, bacitracin, cystamine, hypotaurine, P1, and PACMA 31)[31–35] on the trafficking of the misfolded Z-AAT variant (Fig. S5). We detected a statistically significant increase in trafficking and secretion of Z-AAT only in response to treatment with cystamine (Fig. S5A).

Driven by the positive outcome of the cystamine treatment results, we next investigated the possibility that cysteamine, the reduced form of cystamine, could also rescue Z-AAT trafficking and secretion. Cysteamine is an FDA-approved drug for the treatment of cystinosis, the most common hereditary cause of renal Fanconi syndrome in children,[36,37] with a known safety profile and good bioavailability upon oral administration. In agreement, we did not observe a lag of proliferation or toxicity associated with cysteamine treatment in Z-IB3 cells (Fig. 5A).

To better characterise the cysteamine-mediated correction of Z-AAT, both Z-Huh7 and Z-IB3 cells were treated with increasing concentrations of cysteamine for 24 h (Fig. 6A). Cysteamine improved Z-AAT secretion in a dose-dependent manner, and correction was observed at concentrations as low as 100 μM, with maximal response at 250 μM (Fig. 6A). We performed a treatment time course using the optimal 250 μM cysteamine dose to analyse the kinetics of cysteamine-mediated rescue of Z-AAT secretion. We observed an increased level of Z-AAT secretion after only 2 h of treatment and a maximal response after 18 h of treatment (Fig. S6B). Thus, at the optimal dose and time (250 μM and 18 h), we showed that cysteamine treatment led to a significant increase in Z-AAT secretion (Fig. 5B and Fig. S6C) and strongly reduced the formation of Z-AAT aggregates. This is shown by the marked decrease of Z-AAT in the insoluble fraction following cysteamine treatment (Fig. 5C and Fig. S6D) in Z-IB3 and Z-Huh7 cells. This suggests that cysteamine treatment could provide better elimination of the insoluble and hepatotoxic forms of Z-AAT.

Cysteamine reduces the oxidative stress associated with Z-AATD-mediated liver toxicity

In light of the aforementioned beneficial effects of PDI silencing and cysteamine treatment on Z-AAT aggregation and secretion, we examined if these 2 treatments could also have beneficial outcomes on autophagy and ER stress induction.[21,38,39] Following

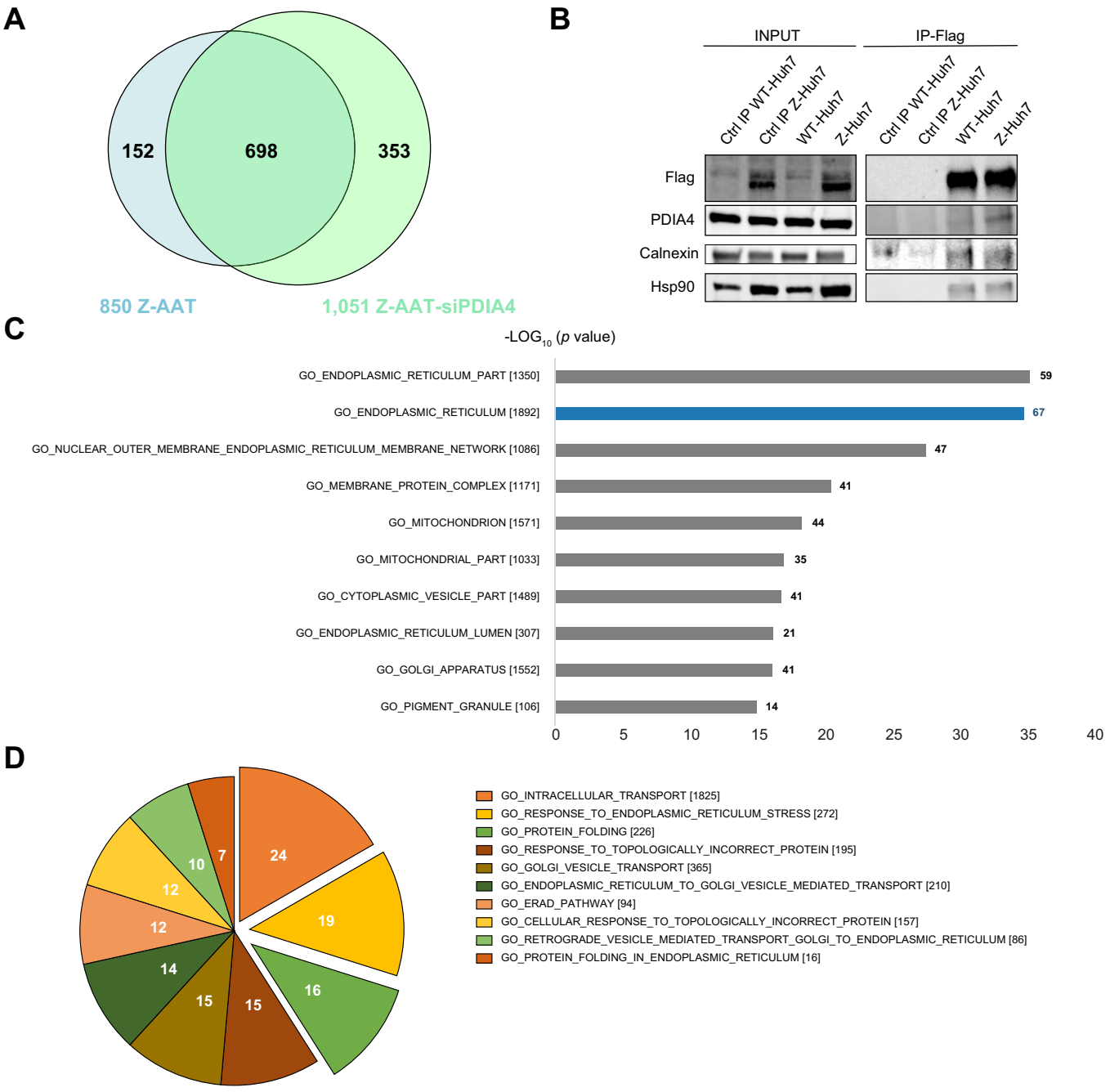

Fig. 4. Dynamic changes of the Z-AAT interactome upon PDIA4 silencing. (A) Proportional Venn diagram depicting the overlap of Z-AAT interactions affected by scramble (scr) control (Z-AAT-blue) or siRNA-mediated silencing of PDIA4 (Z-AAT-siPDIA4/green). This Venn diagram indicates the number of proteins significantly regulated between the Z-AAT interactome upon scr (Z-AAT-blue – 850 interactors) and Z-AAT interactome upon PDIA4 silencing (Z-AAT-siPDIA4/green – 1,051 interactors), core interactome (698 interactors) and those detected only in Z-AAT (152 interactors) or Z-AAT-siPDIA4-IPs (353 interactors). Flag-IPs were performed into Huh7 cell lines that stably express Z-AAT Flag tag and data are representative of at least 3 independent IP experiments per conditions. (B) Immunoblot analysis of AAT (WT and Z), PDIA4, calnexin, and Hsp90 before (input) and after immunoprecipitation of flag tag (IP Flag) into Huh7 cell lines that stably express WT or Z-AAT flag tag. Controls IP (Ctrl IP) correspond to the beads mixed with lysate; from WT or Z-Huh7; without any antibody. Calnexin is used here as a positive control of AAT co-IPs. Data are representative of at least 3 independent IP experiments per conditions. (C) Gene set enrichment: results of the gene ontology (GO) biological processes enrichment for the 353 interactors detected only in Z-AAT-siPDIA4-IPs and significantly differentially expressed between Z-AAT and Z-AAT-siPDIA4-IPs (adjusted *p* value: $p < 0.005$). The x-axis represents the negative log10 *p* value. The number of each graph bars corresponds to the fraction of proteins within the set of 70 proteins that have the corresponding GO function. (D) GO biological processes enrichment for the 67 interactors detected only in the corresponding GO_endoplasmic reticulum [1,892] shown in (C). AAT, alpha 1-antitrypsin; IP, immunoprecipitation; PDIA4, protein disulfide isomerase family A member 4/ERP70/ERP72; WT, wild-type; Z-AAT, alpha 1-antitrypsin Z variant.

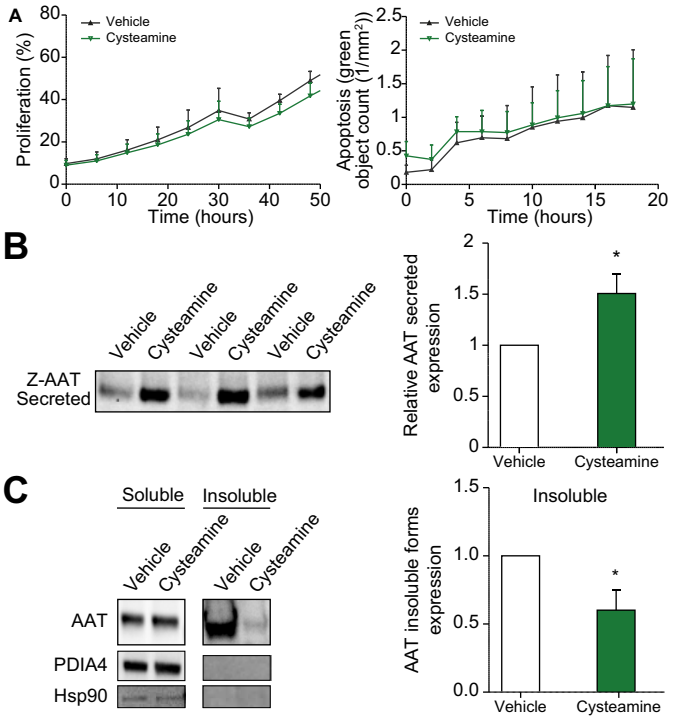

Fig. 5. Effect of cysteamine treatment on Z-AAT secretion and aggregation features. (A) IncuCyte® proliferation assay of Z-AAT IB3 (left) cells following DMSO/vehicle (black) or with 250 μM of cysteamine (green) treatments. Proliferation was quantified in real time using the IncuCyte® live-cell analysis system (see Materials and methods section). IncuCyte® apoptosis assay (right) was performed on Z-IB3 cells upon DMSO/vehicle (black) or cysteamine (green) treatments. Cells were treated with cysteamine at 250 μM for 18 h and IncuCyte® caspase-3/7 green reagent was added into the medium and cells were then incubated all along the indicated time (h). The IncuCyte® caspase-3/7 apoptosis assay green reagent couples the activated caspase-3/7 recognition motif (DEVD) to NucView™ 488, a DNA intercalating dye to enable quantification of apoptosis over time (see Supplementary Materials and methods section). Apoptotic cells were quantified in real time using the IncuCyte® live-cell analysis system. (B) Immunoblot analysis (above) of AAT expression from culture media following treatment of Z-Huh7 cells with 250 μM of cysteamine for 18 h and quantification (below) of Z-AAT secreted forms following DMSO/vehicle (white graph) or with 250 μM of cysteamine (green graph) treatments. Data denote the fold change in the protein expression of the indicated Z-AAT secreted form relative to DMSO/vehicle treatment (mean ± SD, n = 3 independent experiments). (C) Immunoblot analysis of Z-AAT, PDIA4 and Hsp90 proteins expression in cell lysate soluble and insoluble (pellet) fractions upon DMSO/vehicle or with 250 μM of cysteamine treatments in Z-IB3 cells and quantification of Z-AAT insoluble forms following DMSO/vehicle (white graph) or with 250 μM of cysteamine (green graph) treatments. Data denote the fold change in the protein expression of the indicated Z-AAT aggregated/insoluble form relative to DMSO/vehicle treatment (mean ± SD, n = 3 independent experiments). *p <0.05 as determined by 2-tailed t test using DMSO/vehicle as reference. AAT, alpha 1-antitrypsin; PDIA4, protein disulfide isomerase family A member 4/ERP70/ERP72; Z-AAT, alpha 1-antitrypsin Z variant.

PDIA4 silencing or cysteamine treatments in our 2 cell line models used to study *AATD*, we did not see a change in the 2 standard markers used to assess autophagy[40]: p62 (autophagy substrate) and LC3 cleavage (autophagosome marker) (Fig. S7). We obtained the same results when we examined the ability of these treatments to reduce the induction of ER stress/unfolded protein response (Fig. S8). Briefly, even if we noted a reduction in BiP/Grp78 expression level after co-treatment with tunicamycin and cysteamine or tunicamycin and PDIA4 silencing in Z-Huh7 cells, these decreases were not statistically significant (Fig. S8). In all, these results suggest that PDIA4 silencing and cysteamine treatments do not have significant effects on autophagy or ER stress induction.

Given the known antioxidant role of cysteamine and the role of PDIA4 in oxidative stress,[12,41] we examined next whether these 2 treatments could have a beneficial effect on AATD-mediated oxidative stress.[15] First, we directly measured the level of hydrogen peroxide ROS in our cell line models (Fig. 6A). We showed a clear decrease in hydrogen peroxide level after cysteamine treatment of WT and Z-AAT expressing cells (Fig. 6A, left). This same result was confirmed upon PDIA4 silencing. We observed a statistically significant decrease in hydrogen peroxide level following PDIA4 knockdown in cells exclusively expressing the Z variant (Fig. 6A, right). These results suggest a therapeutic potential for PDIA4 silencing and cysteamine treatment in oxidative stress in AATD-mediated disease progression.

Additionally, we examined the effects of these two treatments on the expression of 86 genes related to oxidative stress by qPCR array in WT and Z-IB3 cells. Ten genes (CCL5, CYGB, NCF2, PTGS1/2, AKR1C2, GPX2, GCLM, SEPP1, and GCLC) exhibited a differential mRNA expression in Z-IB3 cells compared with WT-IB3 cells (Fig. 6B). From this short list of genes, we detected 3 genes (CYGB, AKR1C2, SEPP1) with altered expression upon PDIA4 silencing and 6 genes (CCL5, NCF2, CYGB, GCLM, SEPP1, GCLC) upon cysteamine treatment. The expression of these latter 5 genes was similar to or equal to those observed in WT-IB3 cells following treatments (Fig. 6B). Overall, these results suggest that PDIA4 contributes to oxidative stress associated with Z-AATD and that cysteamine treatment restores more physiological levels of oxidative stress/ROS. Cysteamine should therefore be considered for treatment of AATD-mediated liver disease.

Discussion

In this study, we provide original evidence showing that PDIA4/ERp72 is important in AATD-mediated liver disease. We report the improvement of Z-AAT trafficking and secretion, along with a marked decrease in Z-AAT aggregates in response to both PDIA4 silencing and treatment with a PDI inhibitor known as cysteamine. The mechanism of action of this PDIA4 knockdown-mediated correction is in part attributable to the modulation of the interaction of Z-AAT with new components of the ER proteostasis network that promote Z-AAT folding and secretion. Finally, we report that treatment with cysteamine can improve Z-AAT biogenesis (secretion and Z aggregation) and reduce the oxidative stress involved in AAT-mediated liver disease.

Members of the PDI superfamily comprise a multi-domain structure varying in length, domain arrangement, and substrate specificity.[11] They all however contain a thioredoxin (TRX)-like domain and a KDEL (ER-retrieval signal) sequence.[9] PDIA4 is one of the largest PDI family members and comprises 645 amino acids and 5 TRX domains, including 3 Cys-Gly-His-Cys (CGHC) classical active site motifs.[11] The role of the PDIA4 domain in Z-AAT interaction and correction requires further investigation. PDIA4 is a part of the chaperone multi-protein complex that includes Hsp70, BiP, Grp94, PDI, and ERp29.[42] Moreover, PDIA4 sequence analysis has revealed that it is most highly similar to PDIA3/Erp57, with approximately 40% sequence identity.[11] This observation consolidates our results showing that: (i) PDIA3

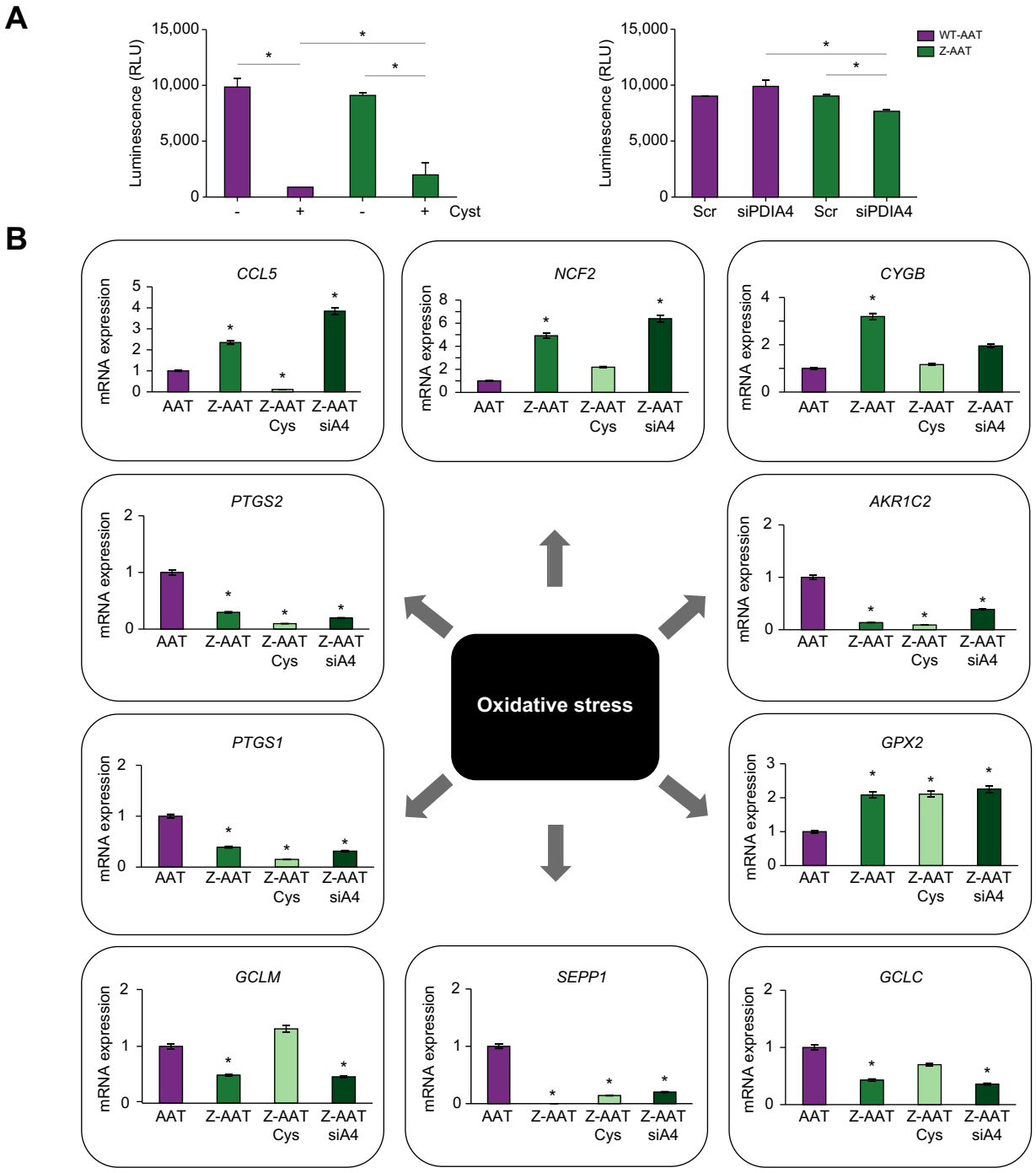

Fig. 6. Oxidative stress and AATD. (A) Cysteamine treatment (Cyst) and PDIA4 silencing (si PDIA4) caused a significant decrease in cellular H2O2 levels in Z-AAT (black bars) expressing cells compared with WT-AAT (purple bars) expressing cell lines. Each bar represents mean ± SD of three independent experiments per conditions (*p <0.05). (B) qPCR analysis of the effect of Z-AAT protein expression, siRNA-mediated silencing of PDIA4 (siA4) and 250 μM cysteamine treatment on the mRNA levels of 10 genes related to oxidative stress in Z-IB3 cells. The data are presented as a fold change in expression relative to WT-IB3 (mean ± SD, n = 3) and genes with a statistically significant difference between WT-AAT and Z-AAT in expression (p <0.05), as determined by Student's t test, are shown. AAT, alpha 1-antitrypsin; AATD, alpha 1-antitrypsin deficiency; PDIA4, protein disulfide isomerase family A member 4/ERP70/ERP72; siRNA, small RNA interference; WT, wild-type; Z-AAT, alpha 1-antitrypsin Z variant.

interacts with Z-AAT, (ii) PDIA3 silencing can rescue Z-AAT trafficking and secretion (Fig. 2A), and (iii) as observed for PDIA4, PDIA3 expression is upregulated in adult ZZ patients (Fig. 1B).

Regarding the pathology, Z-AAT-mediated liver disease is highly variable with a prevalence of intermediate liver fibrosis (F ≥ 2) in ZZ adults of approximately 30–40%,[6,43] and a prevalence of advanced liver fibrosis, and consequently life-threatening liver diseases (cirrhosis, fatty liver, HCC), of approximately 10% in ZZ patients.[2,7,44–46] Liver disease in adults is still under-recognised and under-diagnosed owing to the fact that biochemical and

histopathological analyses can be similar to those underlying other liver diseases.[6,45] Thus, our data (Fig. 3 and Fig. S2B and Table S3) suggest that PDIA4 could represent a potential marker or diagnostic tool (using IHC or proteomic analysis) for Z-AATD-mediated severe liver disease in adults. This hypothesis supports the need of larger scale screening of PDIA4 expression in patients with AATD as well as in patients presenting other liver diseases.

Several questions regarding Z-AATD-mediated liver disease remain unanswered.[45] Here, we complete the current knowledge with respect to Z-AAT aggregate formation and the role of PDIs in ZZ-AATD-mediated severe liver disease in adults. Indeed, based on our proteomic analysis (Fig. 1A), the proteins found upregulated in adult samples were significantly enriched in the 'Protein processing in the endoplasmic reticulum' network (Fig. S1A). This is conversely to the 33 proteins upregulated in the paediatric samples that enriched preferentially in peroxisome or metabolic networks (Fig. S9 and Table S2). This result is in agreement with the hypothesis that AATD most frequently causes liver disease in adults by similar mechanisms underlying age-dependent degenerative diseases, and more rarely in children via powerful modifiers.[19] This in turn explains why PDIs are specifically upregulated in the hepatocytes of adult ZZ patients and not in paediatric ZZ patients.

It is obvious that genetic modifiers and/or environmental factors play a significant role in the development of Z-AATD-mediated liver disease, but these modifiers still remain to be fully identified.[21,45,47–49] Given the important role of PDIA4 and potentially other PDIs, such as PDIA3, it would be interesting in a subsequent study to sequence the genes encoding PDIs. This could potentially identify mutations and/or modifications underlying the variability observed in the liver disease.

Mechanistically, we show that the correction of Z-AAT trafficking and secretion following PDIA4 inhibition is at least partly mediated by promoting its interaction with key ER components. Indeed, detailed analysis of this specific interactome identified novel interactors of Z-AAT involved in ER protein folding and trafficking. Interestingly, many of the proteins that differentially bind Z-AAT upon PDIA4 silencing have already been implicated in other misfolding diseases. We noticed differential binding of SURF4, PDIA4, and FKBP10 proteins to Z-AAT in patients with AATD, and these proteins are also involved in CF mediated by ΔF508-CFTR.[28] This supports the idea that similar disease mechanisms could underlie these 2 rare genetic diseases, suggesting that CF and AATD could be studied side-by-side in the same research project. In addition, FKBP10 is a molecular chaperone located in the ER[50] and our data suggest that FKBP10 is a key component of the ER proteostasis network, mediating the correct folding and maturation of Z-AAT. Therefore, FKBP10, and potentially other FKBP members, could be new and important targets for consideration in the therapeutic management of AATD.

We also describe for the first time the Z-AAT interactome and the identification of 698 individual Z-AAT interactors. Based on the analysis of this 'core' interactome, we demonstrated that PDIA4 is able to interact with Z-AAT and not with WT-AAT (Fig. 4B). In light of our previous comment above on CF, PDIA4 is also able to bind to and rescue the trafficking of the most common CFTR mutant, the well-known ΔF508.[28] Together these data suggest that PDIA4 plays a general role in ER retention of misfolded proteins by direct interaction with them. PDIA4 thus represents a key target for the therapeutic treatment of protein misfolding diseases.

To date, there are unfortunately no specific PDIA4 inhibitors, and more generally there is a lack of potent and selective PDI inhibitors under clinical development owing to their uncontrolled off-target toxicity.[11,51] However, our findings here provide evidence that cystamine and cysteamine, the FDA-approved reduced form of cystamine, have significant effects on Z-AAT biogenesis (secretion and aggregation) (Fig. 5 and Figs. S5 and S6). Cysteamine treatment has already been shown to rescue, favour, and conserve the expression of functional ΔF508-CFTR at the epithelial surface of respiratory cells by restoring autophagy in a mouse model and human patients.[52,53] Thus, this inhibitor has already been identified as a candidate drug for the treatment of patients with CF harbouring the ΔF508-CFTR mutation.[52,53] With respect to AATD, we only observed beneficial effects of cysteamine treatment on AATD-mediated oxidative stress (Fig. 6A and B). We did not observe changes in the 2 standard markers used to assess autophagy[40] (p62 [autophagy substrate] and LC3 cleavage [autophagosome marker]) following cystamine or cysteamine treatments (Fig. S7A, B, and E). Conversely to in CF, the autophagic properties of cysteamine did not account for the beneficial effects on Z-AAT biogenesis we observed, suggesting that this treatment effect was indeed linked to PDI inhibition.

We additionally observed that cysteamine treatment and PDIA4 knockdown implicate the regulation of genes related to Z-AAT-mediated oxidative stress. A '2-hit model' was previously postulated to explain the pathogenesis underlying AATD-mediated liver disease. The first 'hit' corresponds to the accumulation of Z-AAT aggregates and the second 'hit' can include oxidative stress. Indeed, in a mouse model of AATD this stress has been considered a contributing factor in the development of AATD-mediated liver disease.[15] In agreement with this, we detected a deregulated expression of 10 genes related to oxidative stress in Z-IB3 versus WT-IB3 cells, and this deregulation was partially improved upon PDIA4 silencing and cysteamine treatment (Fig. 6B). This suggests that PDIA4 induces at least some of the oxidative stress developed in AATD, and it corroborates with the increasing evidence that PDIs cause oxidative stress.[12,54] Thus, it would be interesting to determine next if the role of PDIA4 in the induction of oxidative stress is related to its interaction with Z-AAT and/or to its role in retention of Z-AAT in the ER via aberrant disulfide bond formation.

We found that cysteamine treatment reduced oxidative stress to a greater extent than PDIA4 silencing (Fig. 6A and B). Even though we cannot exclude that other cellular events are involved, this result is consistent with our PDI siRNA screening (Fig. 2A) showing that silencing of different PDI members, such as Erp27, was also able to improve Z-AAT trafficking and secretion. In all, this suggests that pharmacological intervention targeting the PDI family is more relevant for reducing oxidative stress. Overall, our findings are of critical importance as there is currently no specific treatment for AATD-mediated liver disease other than standard supportive care and liver transplantation for severe cases.[2,7]

In conclusion, we demonstrate a role for PDIA4 in the pathogenic retention of Z-AAT in the ER and in oxidative stress associated with Z-AATD, both effects that can be corrected upon PDIA4 silencing and cysteamine treatments. Moreover, after larger scale validation, the use of PDIA4 as an immunomarker or

PDIA4 expression quantification by mass spectrometry could represent potential therapeutic options for the diagnosis of ZZ-AATD in atypical presentations of AATD-mediated liver disease in adults. Overall, our study provides promising advances in the diagnosis, prognosis, and therapeutic management of AATD-mediated liver disease.

Abbreviations

ΔF508-CFTR, most common mutation of CFTR, which deletes phenylalanine508; AAT, alpha 1-antitrypsin; AATD, alpha 1-antitrypsin deficiency; CF, cystic fibrosis; CFTR, cystic fibrosis transmembrane conductance regulator; ER, endoplasmic reticulum; FFPE, formalin-fixed paraffin-embedded; FKBP10, FK506-binding protein (FKBP) isoform 10; HCC, hepatocellular carcinoma; IHC, immunohistochemistry; IP, immunoprecipitation; NHK, null Hong Kong variant of AAT; P4HB, prolyl 4-hydroxylase subunit beta/PDIA1; PDI, protein disulfide isomerase; PDIA3, protein disulfide isomerase family A member 3/ERP57; PDIA4, protein disulfide isomerase family A member 4/ERP70/ERP72; PDIi, PDI inhibitors; ROS, reactive oxygen species; Scr, scramble; siRNA, small RNA interference; SURF4, proteins Surfeit 4; TRX, thioredoxin; TXNDC5, thioredoxin domain containing 5/PDIA15; WT, wild-type; Z-AAT, alpha 1-antitrypsin Z variant; ZZ, *homozygosis* for the *Z* mutant *allele*.

Financial support

This work was funded by ADAAT Alpha1-France (France), association Suisse Alpha-1 (Switzerland), CSL Behring (France), European Association for the Study of the Liver (EASL) Daniel Alagille Award, the University of Bordeaux (France), CNRS (France), and INSERM (France). E. Karatas is supported by a Région Nouvelle-Aquitaine (France), LFB Biomédicaments (France), and an ADAAT Alpha1-France (France) doctoral studentship.

Conflicts of interest

The authors have no potential conflicts (financial, professional, or personal) relevant to the manuscript.

Please refer to the accompanying ICMJE disclosure forms for further details.

Authors' contributions

Study concept and design: MB, EK, AAR. Acquisition of data: MB, EK, CL, NS, JWD, SDT. Analysis and interpretation of data: MB, EK, AAR, CL, NS, JWD, SDT, FS, MR, AL. Statistical analysis: EK, AAR. Technical support: EK, AAR, CL, JWD, NS, SDT. Administrative support: MR, SCF, AL. Provided patient material: MR, SCF, AL. Drafting of manuscript: MB, EK, AAR, CL, JWD, MR, FS. Study supervision: MB. Obtained funding: MB. Critical review and approved the manuscript: all authors.

Data availability statement

The data that support the findings of this study are available on request from the corresponding author.

Acknowledgements

The authors are grateful to Terezinha Robbe for technical help with FKBP10 RNAi. We are very thankful to Dr Violaine Moreau, Dr Arnaud Jabouille, Dr Ritwick Sawarkar, Dr Matthias Feige, and Dr Adrien Rousseau for their helpful discussions and for critical reading of the manuscript.

Supplementary data

Supplementary data to this article can be found online at https://doi.org/10.1016/j.jhepr.2021.100297.

References

[1] Greene CM, Marciniak SJ, Teckman J, Ferrarotti I, Brantly ML, Lomas DA, et al. alpha1-antitrypsin deficiency. Nat Rev Dis Prim 2016;2:16051.
[2] Karatas E, Di-Tommaso S, Dugot-Senant N, Lachaux A, Bouchecareilh M. Overview of alpha-1 antitrypsin deficiency-mediated liver disease. EMJ Hepatol 2019;7.
[3] Ghouse R, Chu A, Wang Y, Perlmutter DH. Mysteries of alpha1-antitrypsin deficiency: emerging therapeutic strategies for a challenging disease. Dis Model Mech 2014;7:411–419.
[4] Gooptu B, Dickens JA, Lomas DA. The molecular and cellular pathology of alpha(1)-antitrypsin deficiency. Trends Mol Med 2014;20:116–127.
[5] Bouchecareilh M, Conkright JJ, Balch WE. Proteostasis strategies for restoring alpha1-antitrypsin deficiency. Proc Am Thorac Soc 2010;7:415–422.
[6] Clark VC, Marek G, Liu C, Collinsworth A, Shuster J, Kurtz T, et al. Clinical and histologic features of adults with alpha-1 antitrypsin deficiency in a non-cirrhotic cohort. J Hepatol 2018;69:1357–1364.
[7] Karatas E, Bouchecareilh M. Alpha 1-antitrypsin deficiency: a disorder of proteostasis-mediated protein folding and trafficking pathways. Int J Mol Sci 2020;21:1493.
[8] Ronzoni R, Berardelli R, Medicina D, Sitia R, Gooptu B, Fra AM. Aberrant disulphide bonding contributes to the ER retention of alpha1-antitrypsin deficiency variants. Hum Mol Genet 2016;25:642–650.
[9] Galligan JJ, Petersen DR. The human protein disulfide isomerase gene family. Hum Genom 2012;6:6.
[10] Lee E, Lee DH. Emerging roles of protein disulfide isomerase in cancer. BMB Rep 2017;50:401–410.
[11] Wang Z, Zhang H, Cheng Q. PDIA4: the basic characteristics, functions and its potential connection with cancer. Biomed Pharmacother 2020;122:109688.
[12] Fernandes DC, Manoel AH, Wosniak Jr J, Laurindo FR. Protein disulfide isomerase overexpression in vascular smooth muscle cells induces spontaneous preemptive NADPH oxidase activation and Nox1 mRNA expression: effects of nitrosothiol exposure. Arch Biochem Biophys 2009;484:197–204.
[13] Papp E, Szaraz P, Korcsmaros T, Csermely P. Changes of endoplasmic reticulum chaperone complexes, redox state, and impaired protein disulfide reductase activity in misfolding alpha1-antitrypsin transgenic mice. FASEB J 2006;20:1018–1020.
[14] Bouchecareilh M, Hutt DM, Szajner P, Flotte TR, Balch WE. Histone deacetylase inhibitor (HDACi) suberoylanilide hydroxamic acid (SAHA)-mediated correction of alpha1-antitrypsin deficiency. J Biol Chem 2012;287:38265–38278.
[15] Marcus NY, Blomenkamp K, Ahmad M, Teckman JH. Oxidative stress contributes to liver damage in a murine model of alpha-1-antitrypsin deficiency. Exp Biol Med (Maywood) 2012;237:1163–1172.
[16] Henriet E, Abou Hammoud A, Dupuy JW, Dartigues B, Ezzoukry Z, Dugot-Senant N, et al. Argininosuccinate synthase 1 (ASS1): a marker of unclassified hepatocellular adenoma and high bleeding risk. Hepatology 2017;66:2016–2028.
[17] Bouyssie D, Hesse AM, Mouton-Barbosa E, Rompais M, Macron C, Carapito C, et al. Proline: an efficient and user-friendly software suite for large-scale proteomics. Bioinformatics 2020;36:3148–3155.
[18] Perez-Riverol Y, Csordas A, Bai J, Bernal-Llinares M, Hewapathirana S, Kundu DJ, et al. The PRIDE database and related tools and resources in 2019: improving support for quantification data. Nucleic Acids Res 2019;47:D442–D450.
[19] Chu AS, Chopra KB, Perlmutter DH. Is severe progressive liver disease caused by alpha-1-antitrypsin deficiency more common in children or adults? Liver Transpl 2016;22:886–894.
[20] Mitchell EL, Khan Z. Liver disease in alpha-1 antitrypsin deficiency: current approaches and future directions. Curr Pathobiol Rep 2017;5:243–252.
[21] Joly P, Vignaud H, Di Martino J, Ruiz M, Garin R, Restier L, et al. ERAD defects and the HFE-H63D variant are associated with increased risk of liver damages in alpha 1-antitrypsin deficiency. PloS One 2017;12:e0179369.
[22] Wang C, Bouchecareilh M, Balch WE. Measuring the effect of histone deacetylase inhibitors (HDACi) on the secretion and activity of alpha-1 antitrypsin. Methods Mol Biol 2017;1639:185–193.
[23] Schmidt BZ, Perlmutter DH. Grp78, Grp94, and Grp170 interact with alpha1-antitrypsin mutants that are retained in the endoplasmic reticulum. Am J Physiol Gastrointest Liver Physiol 2005;289:G444–G455.
[24] Crowe AR, Yue W. Semi-quantitative determination of protein expression using immunohistochemistry staining and analysis: an integrated protocol. Bio Protoc 2019;9:e3465.
[25] Segeritz CP, Rashid ST, de Brito MC, Serra MP, Ordonez A, Morell CM, et al. hiPSC hepatocyte model demonstrates the role of unfolded protein

response and inflammatory networks in alpha1-antitrypsin deficiency. J Hepatol 2018;69:851–860.
[26] Itzel T, Neubauer M, Ebert M, Evert M, Teufel A. Hepamine – a liver disease microarray database, visualization platform and data-mining resource. Sci Rep 2020;10:4760.
[27] Boyault S, Rickman DS, de Reynies A, Balabaud C, Rebouissou S, Jeannot E, et al. Transcriptome classification of HCC is related to gene alterations and to new therapeutic targets. Hepatology 2007;45:42–52.
[28] Pankow S, Bamberger C, Calzolari D, Martinez-Bartolome S, Lavallee-Adam M, Balch WE, et al. F508 CFTR interactome remodelling promotes rescue of cystic fibrosis. Nature 2015;528:510–516.
[29] Hutt DM, Roth DM, Chalfant MA, Youker RT, Matteson J, Brodsky JL, et al. FK506 binding protein 8 peptidylprolyl isomerase activity manages a late stage of cystic fibrosis transmembrane conductance regulator (CFTR) folding and stability. J Biol Chem 2012;287:21914–21925.
[30] Inoue T, Tsai B. The Grp170 nucleotide exchange factor executes a key role during ERAD of cellular misfolded clients. Mol Biol Cell 2016;27:1650–1662.
[31] Hoffstrom BG, Kaplan A, Letso R, Schmid RS, Turmel GJ, Lo DC, et al. Inhibitors of protein disulfide isomerase suppress apoptosis induced by misfolded proteins. Nat Chem Biol 2010;6:900–906.
[32] Dickerhof N, Kleffmann T, Jack R, McCormick S. Bacitracin inhibits the reductive activity of protein disulfide isomerase by disulfide bond formation with free cysteines in the substrate-binding domain. FEBS J 2011;278:2034–2043.
[33] Xu S, Butkevich AN, Yamada R, Zhou Y, Debnath B, Duncan R, et al. Discovery of an orally active small-molecule irreversible inhibitor of protein disulfide isomerase for ovarian cancer treatment. Proc Natl Acad Sci U S A 2012;109:16348–16353.
[34] Fujita I, Nobunaga M, Seki T, Kurauchi Y, Hisatsune A, Katsuki H. Cystamine-mediated inhibition of protein disulfide isomerase triggers aggregation of misfolded orexin-A in the Golgi apparatus and prevents extracellular secretion of orexin-A. Biochem Biophys Res Commun 2017;489:164–170.
[35] Ge J, Zhang CJ, Li L, Chong LM, Wu X, Hao P, et al. Small molecule probe suitable for in situ profiling and inhibition of protein disulfide isomerase. ACS Chem Biol 2013;8:2577–2585.
[36] Elmonem MA, Veys KR, Soliman NA, van Dyck M, van den Heuvel LP, Levtchenko E. Cystinosis: a review. Orphanet J Rare Dis 2016;11:47.
[37] Medic G, van der Weijden M, Karabis A, Hemels M. A systematic literature review of cysteamine bitartrate in the treatment of nephropathic cystinosis. Curr Med Res Opin 2017;33:2065–2076.
[38] Hidvegi T, Ewing M, Hale P, Dippold C, Beckett C, Kemp C, et al. An autophagy-enhancing drug promotes degradation of mutant alpha1-antitrypsin Z and reduces hepatic fibrosis. Science 2010;329:229–232.
[39] Ordonez A, Snapp EL, Tan L, Miranda E, Marciniak SJ, Lomas DA. Endoplasmic reticulum polymers impair luminal protein mobility and sensitize to cellular stress in alpha1-antitrypsin deficiency. Hepatology 2013;57:2049–2060.
[40] Klionsky DJ, Abdelmohsen K, Abe A, Abedin MJ, Abeliovich H, Acevedo Arozena A, et al. Guidelines for the use and interpretation of assays for monitoring autophagy (3rd edition). Autophagy 2016;12:1–222.
[41] Parakh S, Atkin JD. Novel roles for protein disulphide isomerase in disease states: a double edged sword? Front Cell Dev Biol 2015;3:30.
[42] Meunier L, Usherwood YK, Chung KT, Hendershot LM. A subset of chaperones and folding enzymes form multiprotein complexes in endoplasmic reticulum to bind nascent proteins. Mol Biol Cell 2002;13:4456–4469.
[43] Hamesch K, Mandorfer M, Pereira VM, Moeller LS, Pons M, Dolman GE, et al. Liver fibrosis and metabolic alterations in adults with alpha1 antitrypsin deficiency caused by the Pi*ZZ mutation. Gastroenterology 2019;157. 705–19.e18.
[44] Tanash HA, Piitulainen E. Liver disease in adults with severe alpha-1-antitrypsin deficiency. J Gastroenterol 2019;54:541–548.
[45] Bouchecareilh M. Alpha-1 antitrypsin deficiency-mediated liver toxicity: why do some patients do poorly? What do we know so far? Chron Obstr Pulm Dis 2020;7:172–181.
[46] Eriksson S, Carlson J, Velez R. Risk of cirrhosis and primary liver cancer in alpha 1-antitrypsin deficiency. N Engl J Med 1986;314:736–739.
[47] Pan S, Huang L, McPherson J, Muzny D, Rouhani F, Brantly M, et al. Single nucleotide polymorphism-mediated translational suppression of endoplasmic reticulum mannosidase I modifies the onset of end-stage liver disease in alpha1-antitrypsin deficiency. Hepatology 2009;50:275–281.
[48] Joly P, Lachaux A, Ruiz M, Restier L, Belmalih A, Chapuis-Cellier C, et al. SERPINA1 and MAN1B1 polymorphisms are not linked to severe liver disease in a French cohort of alpha-1 antitrypsin deficiency children. Liver Int 2017;37:1608–1611.
[49] Ruiz M, Lacaille F, Berthiller J, Joly P, Dumortier J, Aumar M, et al. Liver disease related to alpha1-antitrypsin deficiency in French children: the DEFI-ALPHA cohort. Liver Int 2019;39:1136–1146.
[50] Ishikawa Y, Vranka J, Wirz J, Nagata K, Bachinger HP. The rough endoplasmic reticulum-resident FK506-binding protein FKBP65 is a molecular chaperone that interacts with collagens. J Biol Chem 2008;283:31584–31590.
[51] Gonzalez-Santiago L, Alfonso P, Suarez Y, Nunez A, Garcia-Fernandez LF, Alvarez E, et al. Proteomic analysis of the resistance to aplidin in human cancer cells. J Proteome Res 2007;6:1286–1294.
[52] De Stefano D, Villella VR, Esposito S, Tosco A, Sepe A, De Gregorio F, et al. Restoration of CFTR function in patients with cystic fibrosis carrying the F508del-CFTR mutation. Autophagy 2014;10:2053–2074.
[53] Luciani A, Villella VR, Esposito S, Gavina M, Russo I, Silano M, et al. Targeting autophagy as a novel strategy for facilitating the therapeutic action of potentiators on DeltaF508 cystic fibrosis transmembrane conductance regulator. Autophagy 2012;8:1657–1672.
[54] de APAM, Verissimo-Filho S, Guimaraes LL, Silva AC, Takiuti JT, Santos CX, et al. Protein disulfide isomerase redox-dependent association with p47(phox): evidence for an organizer role in leukocyte NADPH oxidase activation. J Leukoc Biol 2011;90:799–810.